

FORMATION OF ${}_{\Lambda}^{15}\text{N}$ HYPERNUCLEUS IN J-PARC E07 EXPERIMENT

Htaik Nandar Kyaw¹, Hnin Yee Hlaing²

Abstract

In this research, a single- Λ hypernucleus which is detected in J-PARC E07 nuclear emulsion experiment is analyzed by relativistic kinematics. The ranges and position angles of charged particle tracks are measured in nuclear emulsion. Neutral particle emission in the decay products is checked by calculating the dot product of direction vector of hyperfragment and total momentum of decay products. The possible decay modes of single- Λ hypernucleus are considered and Q-values are calculated. Total energies of each decay product are obtained by range-energy relation and momentum conservation. The acceptable decay modes are chosen by comparing Q-values and total energy. Then, mass of possible hypernuclei is calculated by mass-energy relation. According to our analysis, a single- Λ hypernucleus is uniquely identified as ${}_{\Lambda}^{15}\text{N}$ which follows the ${}_{\Lambda}^{15}\text{N} \rightarrow {}_4^9\text{Be} + {}_2^3\text{He} + \text{d} + \text{n}$ decay mode with the mass $14141.58 \pm 0.19 \text{ MeV}/c^2$ and binding energy $14.31 \pm 0.19 \text{ MeV}$.

Keywords: Single- Λ hypernucleus, nuclear emulsion, relativistic kinematics, J-PARC

Introduction

Hypernuclei are bound systems of nucleons with one or more hyperons. Hyperons are unstable particles with a mean lifetime of the order of 10^{-10}s . In the family of hyperons, Λ is the lightest particle and it can stay in contact with nucleons inside nuclei and form hypernuclei. If a nucleus contains one Λ hyperon, it is said to be a single- Λ hypernucleus and a nucleus which made up of two Λ hyperons in addition to nucleons is called a double- Λ hypernucleus. Hyperons are free from Pauli's exclusion principle and they can travel deep inside of the nuclear medium until the core region of strange matter such as neutron stars that may exist in distant parts of the universe. The theoretical motivation of hypernuclear physics is to understand the baryon-baryon interaction in a unified way. Under the title of baryon-baryon interaction, nucleon-nucleon interaction can be studied by ordinary nuclei, hyperon-nucleon interaction can be studied by single- Λ hypernuclei and hyperon-hyperon interaction can also be studied by double- Λ hypernuclei. The experimental motivation of hypernuclear physics is to draw the three dimensional nuclear chart with number of protons, number of neutrons and strangeness. Therefore, more hypernuclei events are expected and hypernuclei searching experiments such as KEK-PS E176 and KEK-PS E373 are carried out at Japanese High Energy Accelerator Research Organization using $p(K^-, K^+)\Xi^-$ reaction .

The J-PARC E07 experiment, which stands for Japan Accelerator Research Complex, is aimed to improve the roles of material science, life science, nuclear physics and particles physics, especially in astrophysics. The main purposes of this experiment are to detect about 10,000 Ξ^- stopped events by the hybrid emulsion method, automatic scanning method, combining the emulsion and counters and to identify clearly and accurately double hypernuclei. The J-PARC E07 experiment was performed at K 1.8 beam line in the J-PARC Hadron Experimental facility in 2016. This 1.8 GeV/c momentum was chosen to maximize the Ξ stopping yield in the emulsion. The emulsion scanning of the E07 experiment is ongoing now. At present, twice the statistics for Ξ^- stopping events than that of KEK-PS E373 experiment has been scanned. More than ten events

¹ Dr, Lecturer, Department of Physics, Defence Services Academy

² Assistant Lecturer, Captain, Department of Physics, Defence Services Academy

of double and twin- Λ hypernuclei have been observed up to the present. Further impressive events are expected to be observed in the next future.

In this research, a single- Λ hypernucleus event of J-PARC E07 experiment will be analyzed. The experimental data were supported by Professor Nakazawa who is the spokesperson of this experiment from Gifu University in Japan.

Analysis of Single- Λ Hypernucleus Event

Event Description

The analyzed single- Λ hypernucleus event is detected in module #75, plate #3 of J-PARC E07 experiment. The photograph and schematic diagram of analyzed event are presented in figure 1. In the analyzed event, a Ξ^- hyperon is captured by the emulsion nucleus at point A from which two charged particles tracks #1 and #2 are emitted. At point B, the particle of track #1 showed the topology of decayed into three charged particles track #3, track #4 and track #5. This event has two vertex points; one production vertex A and one decayed vertex B. Therefore, the particle of track #1 can be identified as single- Λ hypernucleus. The measured ranges and emitted angles are expressed in table 1.

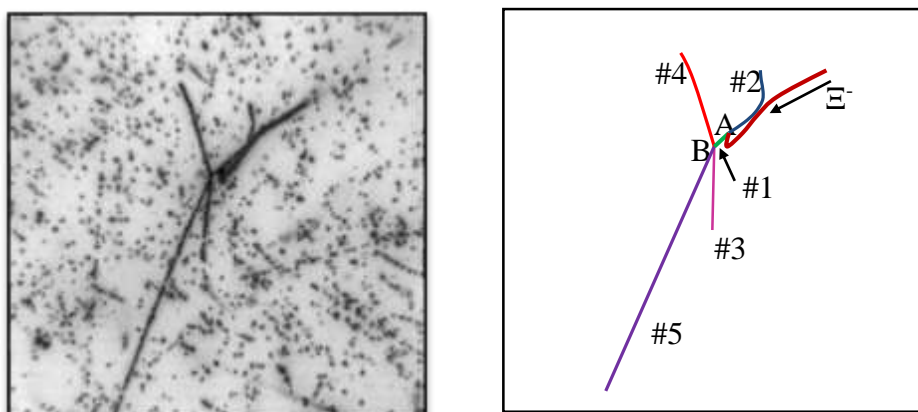


Figure 1 Photographs and schematic diagram of analyzed single- Λ hypernucleus in nuclear emulsion of J-PARC E07 experiment

Table 1 Measured ranges of hypernucleus track #1 and charged particle decay products

| Vertex | Track | Range (μm) | θ (degree) | ϕ (degree) | Remark |
|--------|-------|-------------------------|-------------------|------------------|--------------------------------|
| A | #1 | 1.78 ± 0.00 | 87.09 ± 0.03 | 32.55 ± 0.31 | Single- Λ hypernucleus |
| | #2 | 12.52 ± 0.00 | 94.59 ± 0.06 | 63.18 ± 0.24 | |
| B | #3 | 13.65 ± 0.00 | 80.03 ± 0.09 | 85.91 ± 0.52 | |
| | #4 | 14.67 ± 0.00 | 85.16 ± 0.04 | 69.76 ± 0.20 | |
| | #5 | 101.11 ± 0.04 | 85.24 ± 0.07 | 64.45 ± 0.23 | |

Checking the Neutral Particles Emission at Point B

Present analysis is started from point B and possible decay modes have to choose at point B. At point B, track #1 single- Λ hypernucleus decays into charged particle tracks #3, #4 and #5. So, it is necessary to know neutral particle emission at point B and checked by calculating the dot product of direction vector of hyperfragment and total momentum of decay products such as

$$\cos\theta = \frac{\vec{V}_{HF} \cdot \vec{p}_{total}}{|\vec{V}_{HF}| \cdot |\vec{p}_{total}|} \tag{1}$$

where, \vec{V}_{HF} = the direction vector of hyperfragment

\vec{p}_{total} = the total momentum of the emitted tracks

If the angle θ becomes zero, there is no neutron emission. It means that the total momentum is zero and other neutral particles cannot be emitted at point B. If the angle θ has some value, the neutral particles will be emitted at point B. According to our calculation, the angle θ value is 39.56° and not equal to zero. So, we can consider that not only three charged particles tracks #3, #4 and #5 but also neutral particles can be emitted at the vertex point B and decay modes of single- Λ hypernucleus track #1 will be obtained.

Choosing the Possible Decay Modes at Point B

At point B, a single- Λ hypernucleus (track #1) is decayed into three charged particles and one or more neutral particles as follow.

$${}^{\Lambda}Z(\text{Track \#1}) \rightarrow \text{Track \#3} + \text{Track \#4} + \text{Track \#5} + \text{neutral particle (s)} \tag{2}$$

Therefore, possible decay modes of single- Λ hypernucleus track #1 are chosen according to equation 2. Firstly, internal structures of possible single- Λ hypernuclei are considered. Track #1 decays into decay products of three charged particle tracks and neutral particles, the possible hypernucleus must be chosen ${}^{14}_{\Lambda}C$ to ${}^{15}_{\Lambda}N$.

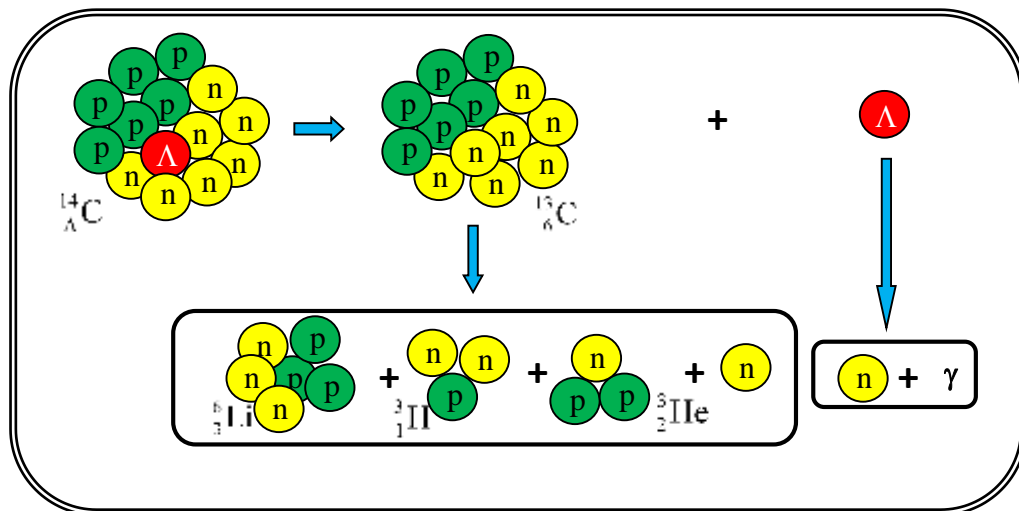


Figure 2 Decay of ${}^{14}_{\Lambda}C$ hypernucleus into three charged particles and two neutral particles

According to figure 2, a ${}^{14}_{\Lambda}C$ hypernucleus consists of 6 protons, 1 Λ hyperon and 7 neutrons (figure 2). It means that a Λ hyperon combines with a core nucleus ${}^{13}_6C$ to form a C^{14} hypernucleus. In the analyzed event, a single- Λ hypernucleus has 3 charged particle decay products and it is assumed that a core nucleus decays into three charged particles Li^6 , H^3 and He^3 . Due to the dot product of hyperfragment direction vector and total momentum of decay products, neutral particle emission at point B is observed. Therefore, the possible decay mode becomes,



Similarly, all possible decay modes are chosen and 85 possible decay modes are obtained.

Calculation of Q-values and Total Energy at Point B

To check the possible decay modes that we have chosen in section 3.6.1 are energetically possible or not, the Q-values at point B are calculated. The Q-value is defined as the energy released or absorbed during the nuclear reaction. If the calculated Q-value is positive, it is defined as an exoergic reaction. If so reaction is energetically possible. If the calculated Q-value is negative, it is defined as an endoergic reaction. In this case, the reaction does not energetically possible and is not taken into the consideration for our analysis.

The Q-values of all possible decay modes are calculated by the formula,

$$Q = \sum M_{\text{initial state}} - \sum M_{\text{final state}} \quad (4)$$

$$Q(\text{MeV}) = [M({}_{\Lambda}^A Z)(\text{MeV}/c^2) - \{M(\#3) + M(\#4) + M(\#5) + M(n)\}(\text{MeV}/c^2)]c^2 \quad (5)$$

The lifetime of hypernuclei is very short ($\sim 10^{-10}\text{s}$) and it decays itself without external effects in nuclear emulsion. So, an exoergic reaction is allowed in nuclear emulsion. Moreover, if Q-value is positive, the energy is released and this energy is shared by the decay products. Therefore, only exoergic reaction must be allowed for these decay modes. According to our calculation it is found that the calculated Q-values are all positive and all possible decay modes are taken into consideration to perform analysis.

The kinetic energies of charged particles which are called visible energy (E_{vis}) are obtained by range-energy relation calculation package by measuring its range. The kinetic energies of neutral particles (E_n) are calculated by momentum conservation. Total energy means that the sum of kinetic energies of charged particle decay products and that of neutral particles. If all charged particles are emitted Q-values should be equal to total kinetic energy. If neutral particles are contaminated in the decay products, Q-values should be less than total kinetic energy.

In the present analysis, a single- Λ hypernucleus decays into three charged particles and one or more neutral particles so that we should choose the possible decay modes which have smaller total energy than Q-values. In table 2, the comparisons of calculated Q-values and E_{total} for all possible decay modes are presented. Some decay modes have one neutron emission and some have two neutron emission. The decay modes which have more than two neutrons emission are rejected because of very small and negative Q-values.

Table 2 Comparison of Q-values and total energy for all possible decay modes at point B

| No. | Possible Decay Modes | Q-value (MeV) | E_{total} (MeV) | Remark |
|-----|---|---------------|--------------------------|------------|
| 1 | ${}_{\Lambda}^{14}\text{C} \rightarrow {}_3^6\text{Li} + {}_1^3\text{H} + {}_2^3\text{He} + 2n$ | 114.98±0.33 | >60.31±0.01 | Acceptable |
| 2 | ${}_{\Lambda}^{14}\text{C} \rightarrow {}_3^6\text{Li} + {}_2^3\text{He} + {}_1^3\text{H} + 2n$ | 114.98±0.33 | >47.749±0.01 | Acceptable |
| 3 | ${}_{\Lambda}^{14}\text{C} \rightarrow {}_1^3\text{H} + {}_3^6\text{Li} + {}_2^3\text{He} + 2n$ | 114.98±0.33 | >62.14±0.01 | Acceptable |
| 4 | ${}_{\Lambda}^{14}\text{C} \rightarrow {}_2^3\text{He} + {}_3^6\text{Li} + {}_1^3\text{H} + 2n$ | 114.98±0.33 | >49.24±0.01 | Acceptable |
| 5 | ${}_{\Lambda}^{14}\text{C} \rightarrow {}_1^3\text{H} + {}_2^3\text{He} + {}_3^6\text{Li} + 2n$ | 114.98±0.33 | >117.28±0.01 | Rejected |
| 6 | ${}_{\Lambda}^{14}\text{C} \rightarrow {}_2^3\text{He} + {}_1^3\text{H} + {}_3^6\text{Li} + 2n$ | 114.98±0.33 | >116.94±0.01 | Rejected |
| 7 | ${}_{\Lambda}^{14}\text{C} \rightarrow {}_3^6\text{Li} + {}_1^3\text{H} + {}_2^4\text{He} + n$ | 135.55±0.33 | 119.54±0.01 | Acceptable |

| No. | Possible Decay Modes | Q-value (MeV) | E _{total} (MeV) | Remark |
|-----|---|---------------|--------------------------|------------|
| 8 | ${}^{14}_{\Lambda}C \rightarrow {}^6_3Li + {}^4_2He + {}^3_1H + n$ | 135.55±0.33 | 85.065±0.01 | Acceptable |
| 9 | ${}^{14}_{\Lambda}C \rightarrow {}^3_1H + {}^6_3Li + {}^4_2He + n$ | 135.55±0.33 | 122.77±0.01 | Acceptable |
| 10 | ${}^{14}_{\Lambda}C \rightarrow {}^4_2He + {}^6_3Li + {}^3_1H + n$ | 135.55±0.33 | 87.38±0.01 | Acceptable |
| 11 | ${}^{14}_{\Lambda}C \rightarrow {}^3_1H + {}^4_2He + {}^6_3Li + n$ | 135.55±0.33 | 208.18±0.01 | Rejected |
| 12 | ${}^{14}_{\Lambda}C \rightarrow {}^4_2He + {}^3_1H + {}^6_3Li + n$ | 135.55±0.33 | 207.26±0.01 | Rejected |
| 13 | ${}^{14}_{\Lambda}C \rightarrow {}^6_3Li + {}^2_1H + {}^4_2He + 2n$ | 129.29±0.33 | >69.62±0.01 | Acceptable |
| 14 | ${}^{14}_{\Lambda}C \rightarrow {}^6_3Li + {}^4_2He + {}^2_1H + 2n$ | 129.29±0.33 | >46.22±0.01 | Acceptable |
| 15 | ${}^{14}_{\Lambda}C \rightarrow {}^2_1H + {}^6_3Li + {}^4_2He + 2n$ | 129.29±0.33 | >71.55±0.01 | Acceptable |
| 16 | ${}^{14}_{\Lambda}C \rightarrow {}^4_2He + {}^6_3Li + {}^2_1H + 2n$ | 129.29±0.33 | >47.53±0.01 | Acceptable |
| 17 | ${}^{14}_{\Lambda}C \rightarrow {}^2_1H + {}^4_2He + {}^6_3Li + 2n$ | 129.29±0.33 | >118.94±0.01 | Acceptable |
| 18 | ${}^{14}_{\Lambda}C \rightarrow {}^4_2He + {}^2_1H + {}^6_3Li + 2n$ | 129.29±0.33 | >118.32±0.01 | Acceptable |
| 19 | ${}^{14}_{\Lambda}C \rightarrow {}^7_3Li + {}^3_1H + {}^3_2He + n$ | 122.23±0.34 | 108.06±0.01 | Acceptable |
| 20 | ${}^{14}_{\Lambda}C \rightarrow {}^7_3Li + {}^3_2He + {}^3_1H + n$ | 122.23±0.33 | 87.96±0.01 | Acceptable |
| 21 | ${}^{14}_{\Lambda}C \rightarrow {}^3_1H + {}^7_3Li + {}^3_2He + n$ | 122.23±0.33 | 112.05±0.01 | Acceptable |
| 22 | ${}^{14}_{\Lambda}C \rightarrow {}^3_2He + {}^7_3Li + {}^3_1H + n$ | 122.23±0.33 | 91.42±0.01 | Acceptable |
| 23 | ${}^{14}_{\Lambda}C \rightarrow {}^3_1H + {}^3_2He + {}^7_3Li + n$ | 122.23±0.33 | 242.03±0.01 | Rejected |
| 24 | ${}^{14}_{\Lambda}C \rightarrow {}^3_2He + {}^3_1H + {}^7_3Li + n$ | 122.23±0.33 | 241.49±0.01 | Rejected |
| 25 | ${}^{14}_{\Lambda}C \rightarrow {}^7_3Li + {}^2_1H + {}^3_2He + 2n$ | 115.98±0.33 | >63.29±0.01 | Acceptable |
| 26 | ${}^{14}_{\Lambda}C \rightarrow {}^7_3Li + {}^3_2He + {}^2_1H + 2n$ | 115.98±0.33 | >47.64±0.01 | Acceptable |
| 27 | ${}^{14}_{\Lambda}C \rightarrow {}^2_1H + {}^7_3Li + {}^3_2He + 2n$ | 115.98±0.33 | >65.58±0.03 | Acceptable |
| 28 | ${}^{14}_{\Lambda}C \rightarrow {}^3_2He + {}^7_3Li + {}^2_1H + 2n$ | 115.98±0.33 | >49.56±0.01 | Acceptable |
| 29 | ${}^{14}_{\Lambda}C \rightarrow {}^2_1H + {}^3_2He + {}^7_3Li + 2n$ | 115.98±0.33 | >136.50±0.03 | Rejected |
| 30 | ${}^{14}_{\Lambda}C \rightarrow {}^3_2He + {}^2_1H + {}^7_3Li + 2n$ | 115.98±0.33 | >136.09±0.01 | Rejected |
| 31 | ${}^{14}_{\Lambda}C \rightarrow {}^7_3Li + {}^2_1H + {}^4_2He + n$ | 136.54±0.33 | 125.47±0.01 | Acceptable |
| 32 | ${}^{14}_{\Lambda}C \rightarrow {}^7_3Li + {}^4_2He + {}^2_1H + n$ | 136.54±0.33 | 85.40±0.02 | Acceptable |
| 33 | ${}^{14}_{\Lambda}C \rightarrow {}^2_1H + {}^7_3Li + {}^4_2He + n$ | 136.54±0.33 | 129.60±0.01 | Acceptable |
| 34 | ${}^{14}_{\Lambda}C \rightarrow {}^4_2He + {}^7_3Li + {}^2_1H + n$ | 136.54±0.33 | 88.48±0.02 | Acceptable |
| 35 | ${}^{14}_{\Lambda}C \rightarrow {}^2_1H + {}^4_2He + {}^7_3Li + n$ | 136.54±0.33 | 245.19±0.01 | Rejected |
| 36 | ${}^{14}_{\Lambda}C \rightarrow {}^4_2He + {}^2_1H + {}^7_3Li + n$ | 136.54±0.33 | 244.14±0.01 | Rejected |
| 37 | ${}^{14}_{\Lambda}C \rightarrow {}^7_3Li + {}^1_1H + {}^4_2He + 2n$ | 134.32±0.33 | >72.62±0.01 | Acceptable |
| 38 | ${}^{14}_{\Lambda}C \rightarrow {}^7_3Li + {}^4_2He + {}^1_1H + 2n$ | 134.32±0.33 | >46.35±0.01 | Acceptable |

| No. | Possible Decay Modes | Q-value (MeV) | E _{total} (MeV) | Remark |
|-----|--|---------------|--------------------------|------------|
| 39 | ${}^{14}_{\Lambda}\text{C} \rightarrow {}^1_1\text{H} + {}^7_3\text{Li} + {}^4_2\text{He} + 2\text{n}$ | 134.32±0.33 | >74.98±0.01 | Acceptable |
| 40 | ${}^{14}_{\Lambda}\text{C} \rightarrow {}^4_2\text{He} + {}^7_3\text{Li} + {}^1_1\text{H} + 2\text{n}$ | 134.32±0.33 | >48.04±0.01 | Acceptable |
| 41 | ${}^{14}_{\Lambda}\text{C} \rightarrow {}^1_1\text{H} + {}^4_2\text{He} + {}^7_3\text{Li} + 2\text{n}$ | 134.14±0.33 | >138.15±0.01 | Rejected |
| 42 | ${}^{14}_{\Lambda}\text{C} \rightarrow {}^4_2\text{He} + {}^1_1\text{H} + {}^7_3\text{Li} + 2\text{n}$ | 134.14±0.33 | >137.46±0.01 | Rejected |
| 43 | ${}^{14}_{\Lambda}\text{C} \rightarrow {}^7_3\text{Li} + {}^1_1\text{H} + {}^5_2\text{He} + \text{n}$ | 133.42±0.38 | 144.87±0.01 | Rejected |
| 44 | ${}^{15}_{\Lambda}\text{N} \rightarrow {}^9_4\text{Be} + {}^2_1\text{H} + {}^3_2\text{He} + \text{n}$ | 125.93±0.21 | 150.86±0.01 | Rejected |
| 45 | ${}^{15}_{\Lambda}\text{N} \rightarrow {}^9_4\text{Be} + {}^3_2\text{He} + {}^2_1\text{H} + \text{n}$ | 125.93±0.16 | 125.17±0.03 | Acceptable |
| 46 | ${}^{15}_{\Lambda}\text{N} \rightarrow {}^2_1\text{H} + {}^9_4\text{Be} + {}^3_2\text{He} + \text{n}$ | 125.93±0.16 | 158.96±0.01 | Rejected |
| 47 | ${}^{15}_{\Lambda}\text{N} \rightarrow {}^3_2\text{He} + {}^9_4\text{Be} + {}^2_1\text{H} + \text{n}$ | 125.93±0.16 | 132.60±0.03 | Rejected |
| 48 | ${}^{15}_{\Lambda}\text{N} \rightarrow {}^2_1\text{H} + {}^3_2\text{He} + {}^9_4\text{Be} + \text{n}$ | 125.93±0.16 | 448.23±0.02 | Rejected |
| 49 | ${}^{15}_{\Lambda}\text{N} \rightarrow {}^3_2\text{He} + {}^2_1\text{H} + {}^9_4\text{Be} + \text{n}$ | 125.93±0.16 | 447.56±0.02 | Rejected |
| 50 | ${}^{15}_{\Lambda}\text{N} \rightarrow {}^9_4\text{Be} + {}^1_1\text{H} + {}^3_2\text{He} + 2\text{n}$ | 123.70±0.16 | >86.19±0.01 | Acceptable |
| 51 | ${}^{15}_{\Lambda}\text{N} \rightarrow {}^9_4\text{Be} + {}^3_2\text{He} + {}^1_1\text{H} + 2\text{n}$ | 123.70±0.16 | >67.68±0.03 | Acceptable |
| 52 | ${}^{15}_{\Lambda}\text{N} \rightarrow {}^1_1\text{H} + {}^9_4\text{Be} + {}^3_2\text{He} + 2\text{n}$ | 123.70±0.16 | >90.69±0.01 | Acceptable |
| 53 | ${}^{15}_{\Lambda}\text{N} \rightarrow {}^3_2\text{He} + {}^9_4\text{Be} + {}^1_1\text{H} + 2\text{n}$ | 123.70±0.16 | >71.70±0.03 | Acceptable |
| 54 | ${}^{15}_{\Lambda}\text{N} \rightarrow {}^1_1\text{H} + {}^3_2\text{He} + {}^9_4\text{Be} + 2\text{n}$ | 123.70±0.16 | >247.18±0.02 | Rejected |
| 55 | ${}^{15}_{\Lambda}\text{N} \rightarrow {}^3_2\text{He} + {}^1_1\text{H} + {}^9_4\text{Be} + 2\text{n}$ | 123.70±0.16 | >246.70±0.02 | Rejected |
| 56 | ${}^{15}_{\Lambda}\text{N} \rightarrow {}^9_4\text{Be} + {}^1_1\text{H} + {}^4_2\text{He} + \text{n}$ | 144.27±0.16 | 168.58±0.01 | Rejected |
| 57 | ${}^{15}_{\Lambda}\text{N} \rightarrow {}^9_4\text{Be} + {}^4_2\text{He} + {}^1_1\text{H} + \text{n}$ | 144.27±0.16 | 123.37±0.03 | Acceptable |
| 58 | ${}^{15}_{\Lambda}\text{N} \rightarrow {}^1_1\text{H} + {}^9_4\text{Be} + {}^4_2\text{He} + \text{n}$ | 144.27±0.16 | 176.37±0.01 | Rejected |
| 59 | ${}^{15}_{\Lambda}\text{N} \rightarrow {}^4_2\text{He} + {}^9_4\text{Be} + {}^1_1\text{H} + \text{n}$ | 144.27±0.16 | 130.42±0.03 | Acceptable |
| 60 | ${}^{15}_{\Lambda}\text{N} \rightarrow {}^1_1\text{H} + {}^4_2\text{He} + {}^9_4\text{Be} + \text{n}$ | 144.27±0.16 | 451.46±0.02 | Rejected |
| 61 | ${}^{15}_{\Lambda}\text{N} \rightarrow {}^4_2\text{He} + {}^1_1\text{H} + {}^9_4\text{Be} + \text{n}$ | 144.27±0.16 | 450.29±0.02 | Rejected |
| 62 | ${}^{15}_{\Lambda}\text{N} \rightarrow {}^{10}_4\text{Be} + {}^1_1\text{H} + {}^3_2\text{He} + \text{n}$ | 130.51±0.16 | 160.13±0.01 | Rejected |
| 63 | ${}^{15}_{\Lambda}\text{N} \rightarrow {}^{10}_4\text{Be} + {}^3_2\text{He} + {}^1_1\text{H} + \text{n}$ | 130.51±0.16 | 129.53±0.03 | Acceptable |
| 64 | ${}^{15}_{\Lambda}\text{N} \rightarrow {}^1_1\text{H} + {}^{10}_4\text{Be} + {}^3_2\text{He} + \text{n}$ | 130.51±0.16 | 169.52±0.01 | Rejected |
| 65 | ${}^{15}_{\Lambda}\text{N} \rightarrow {}^3_2\text{He} + {}^{10}_4\text{Be} + {}^1_1\text{H} + \text{n}$ | 130.51±0.16 | 138.13±0.03 | Rejected |
| 66 | ${}^{15}_{\Lambda}\text{N} \rightarrow {}^1_1\text{H} + {}^3_2\text{He} + {}^{10}_4\text{Be} + \text{n}$ | 130.51±0.16 | 508.09±0.02 | Rejected |
| 67 | ${}^{15}_{\Lambda}\text{N} \rightarrow {}^3_2\text{He} + {}^1_1\text{H} + {}^{10}_4\text{Be} + \text{n}$ | 130.51±0.16 | 507.29±0.02 | Rejected |
| 68 | ${}^{15}_{\Lambda}\text{N} \rightarrow {}^{10}_5\text{B} + {}^1_1\text{H} + {}^3_1\text{H} + \text{n}$ | 131.04±0.16 | 165.18±0.01 | Rejected |
| 69 | ${}^{15}_{\Lambda}\text{N} \rightarrow {}^{10}_5\text{B} + {}^3_1\text{H} + {}^1_1\text{H} + \text{n}$ | 131.04±0.16 | 154.69±0.01 | Rejected |

| No. | Possible Decay Modes | Q-value (MeV) | E _{total} (MeV) | Remark |
|-----|---|---------------|--------------------------|------------|
| 70 | ${}^{15}_{\Lambda}\text{N} \rightarrow {}^1_1\text{H} + {}^{10}_5\text{B} + {}^3_1\text{H} + \text{n}$ | 131.04±0.16 | 177.28±0.01 | Rejected |
| 71 | ${}^{15}_{\Lambda}\text{N} \rightarrow {}^3_1\text{H} + {}^{10}_5\text{B} + {}^1_1\text{H} + \text{n}$ | 131.04±0.16 | 166.62±0.01 | Rejected |
| 72 | ${}^{15}_{\Lambda}\text{N} \rightarrow {}^1_1\text{H} + {}^3_1\text{H} + {}^{10}_5\text{B} + \text{n}$ | 131.04±0.16 | 648.04±0.02 | Rejected |
| 73 | ${}^{15}_{\Lambda}\text{N} \rightarrow {}^3_1\text{H} + {}^1_1\text{H} + {}^{10}_5\text{B} + \text{n}$ | 131.04±0.16 | 647.78±0.02 | Rejected |
| 74 | ${}^{15}_{\Lambda}\text{N} \rightarrow {}^{10}_5\text{B} + {}^2_1\text{H} + {}^2_1\text{H} + \text{n}$ | 127.01±0.16 | 159.51±0.01 | Rejected |
| 75 | ${}^{15}_{\Lambda}\text{N} \rightarrow {}^2_1\text{H} + {}^{10}_5\text{B} + {}^2_1\text{H} + \text{n}$ | 127.01±0.16 | 171.59±0.01 | Rejected |
| 76 | ${}^{15}_{\Lambda}\text{N} \rightarrow {}^2_1\text{H} + {}^1_1\text{H} + {}^{10}_5\text{B} + \text{n}$ | 127.01±0.16 | 647.84±0.02 | Rejected |
| 77 | ${}^{15}_{\Lambda}\text{N} \rightarrow {}^{11}_5\text{B} + {}^1_1\text{H} + {}^2_1\text{H} + \text{n}$ | 136.24±0.16 | 172.13±0.01 | Rejected |
| 78 | ${}^{15}_{\Lambda}\text{N} \rightarrow {}^{11}_5\text{B} + {}^2_1\text{H} + {}^1_1\text{H} + \text{n}$ | 136.24±0.16 | 167.23±0.01 | Rejected |
| 79 | ${}^{15}_{\Lambda}\text{N} \rightarrow {}^1_1\text{H} + {}^{11}_5\text{B} + {}^2_1\text{H} + \text{n}$ | 136.24±0.16 | 185.87±0.01 | Rejected |
| 80 | ${}^{15}_{\Lambda}\text{N} \rightarrow {}^2_1\text{H} + {}^{11}_5\text{B} + {}^1_1\text{H} + \text{n}$ | 136.24±0.16 | 180.84±0.01 | Rejected |
| 81 | ${}^{15}_{\Lambda}\text{N} \rightarrow {}^1_1\text{H} + {}^2_1\text{H} + {}^{11}_5\text{B} + \text{n}$ | 136.24±0.16 | 728.28±0.02 | Rejected |
| 82 | ${}^{15}_{\Lambda}\text{N} \rightarrow {}^2_1\text{H} + {}^1_1\text{H} + {}^{11}_5\text{B} + \text{n}$ | 136.24±0.16 | 728.16±0.02 | Rejected |
| 83 | ${}^{15}_{\Lambda}\text{N} \rightarrow {}^{11}_5\text{B} + {}^1_1\text{H} + {}^1_1\text{H} + 2\text{n}$ | 134.01±0.16 | >91.57±0.01 | Acceptable |
| 84 | ${}^{15}_{\Lambda}\text{N} \rightarrow {}^1_1\text{H} + {}^{11}_5\text{B} + {}^1_1\text{H} + 2\text{n}$ | 134.01±0.16 | >99.12±0.01 | Acceptable |
| 85 | ${}^{15}_{\Lambda}\text{N} \rightarrow {}^1_1\text{H} + {}^1_1\text{H} + {}^{11}_5\text{B} + 2\text{n}$ | 134.01±0.16 | >394.51±0.02 | Rejected |

According to table 2, 45 possible decay modes are rejected because they have larger total energy than Q-values. In this case, we have found that 40 acceptable decay modes in which E_{total} are consistent with Q value within 3σ value. Therefore, 40 possible decay modes are acceptable and they are taken into considerations to calculate the possible mass and binding energy of single-Λ hypernucleus. In the next section, detailed calculation of possible mass and binding energy will be presented.

Calculation of the mass and binding energy of single-Λ hypernucleus (track #1)

The possible masses of single-Λ hypernucleus are calculated by extracting the kinetic energy of charged particle decay products at point B. At point B, a single-Λ hypernucleus decays into three charged particles and neutral particles. The possible masses of single-Λ hypernucleus can be calculated by using the formula,

$$M({}^{\Lambda}_Z) c^2 = E_3 + E_4 + E_5 + E_n \tag{6}$$

where, M({}^{\Lambda}_Z) = mass of single-Λ hypernucleus

E₃ = the total energy of track #3 = KE₃ + M₃

E₄ = the total energy of track #4 = KE₄ + M₄

E₅ = the total energy of track #5 = KE₅ + M₅

E_n = the total energy of neutron = KE_n + M_n

The binding energy of a single-Λ hypernucleus is calculated by the formula

$$B_{\Lambda} = M(^{\Lambda-1}Z) + M_{\Lambda} - M(^{\Lambda}Z) \quad (7)$$

where, B_{Λ} = binding energy of a single- Λ hypernucleus

$M(^{\Lambda-1}Z)$ = mass of core nucleus

M_{Λ} = mass of Λ hyperon

$M(^{\Lambda}Z)$ = mass of a single- Λ hypernucleus

The total binding energy of any ordinary nucleus involves a vital role in nuclear stability. In hypernuclear physics, hypernuclear binding energies determine Y-N and Y-Y effective interaction strengths. The comparison of our calculated results of masses and binding energies of 40 acceptable single- Λ hypernuclei and previous experimental and theoretical values are expressed in table 3.

Table 3 Calculated mass and binding energy compare with known values

| No. | Possible Decay Modes | Calculated Mass(MeV/c ²) | Known Mass(MeV/c) | Calculated BE(MeV) | Known BE(MeV) |
|-----|---|--------------------------------------|-------------------|--------------------|---------------|
| 1 | ${}^{14}_{\Lambda}C \rightarrow {}^6_3Li + {}^3_1H + {}^3_2He + 2n$ | >13158.36±0.34 | 13213.03±0.33 | <66.81±0.34 | 12.17 ±0.33 |
| 2 | ${}^{14}_{\Lambda}C \rightarrow {}^6_3Li + {}^3_2He + {}^3_1H + 2n$ | >13145.80±0.34 | 13213.03±0.33 | <79.37±0.34 | 12.17 ±0.33 |
| 3 | ${}^{14}_{\Lambda}C \rightarrow {}^3_1H + {}^6_3Li + {}^3_2He + 2n$ | >13160.18±0.34 | 13213.03±0.33 | <64.99±0.34 | 12.17 ±0.33 |
| 4 | ${}^{14}_{\Lambda}C \rightarrow {}^3_2He + {}^6_3Li + {}^3_1H + 2n$ | >13147.29±0.34 | 13213.03±0.33 | <77.88±0.34 | 12.17 ±0.33 |
| 5 | ${}^{14}_{\Lambda}C \rightarrow {}^6_3Li + {}^3_1H + {}^4_2He + n$ | 13197.02±0.34 | 13213.03±0.33 | 28.15±0.34 | 12.17 ±0.33 |
| 6 | ${}^{14}_{\Lambda}C \rightarrow {}^6_3Li + {}^4_2He + {}^3_1H + n$ | 13162.55±0.34 | 13213.03±0.33 | 62.62±0.34 | 12.17 ±0.33 |
| 7 | ${}^{14}_{\Lambda}C \rightarrow {}^3_1H + {}^6_3Li + {}^4_2He + n$ | 13200.25±0.34 | 13213.03±0.33 | 24.92±0.34 | 12.17 ±0.33 |
| 8 | ${}^{14}_{\Lambda}C \rightarrow {}^4_2He + {}^6_3Li + {}^3_1H + n$ | 13164.86±0.34 | 13213.03±0.33 | 60.31±0.34 | 12.17 ±0.33 |
| 9 | ${}^{14}_{\Lambda}C \rightarrow {}^6_3Li + {}^2_1H + {}^4_2He + 2n$ | >13153.36±0.35 | 13213.03±0.33 | <71.81±0.35 | 12.17 ±0.33 |
| 10 | ${}^{14}_{\Lambda}C \rightarrow {}^6_3Li + {}^4_2He + {}^2_1H + 2n$ | >13129.96±0.34 | 13213.03±0.33 | <95.21±0.34 | 12.17 ±0.33 |
| 11 | ${}^{14}_{\Lambda}C \rightarrow {}^2_1H + {}^6_3Li + {}^4_2He + 2n$ | >13155.29±0.34 | 13213.03±0.33 | <69.88±0.34 | 12.17 ±0.33 |
| 12 | ${}^{14}_{\Lambda}C \rightarrow {}^4_2He + {}^6_3Li + {}^2_1H + 2n$ | >13131.27±0.34 | 13213.03±0.33 | <93.90±0.34 | 12.17 ±0.33 |
| 13 | ${}^{14}_{\Lambda}C \rightarrow {}^2_1H + {}^4_2He + {}^6_3Li + 2n$ | >13202.06±0.34 | 13213.03±0.33 | <22.49±0.34 | 12.17 ±0.33 |
| 14 | ${}^{14}_{\Lambda}C \rightarrow {}^4_2He + {}^2_1H + {}^6_3Li + 2n$ | >13202.06±0.34 | 13213.03±0.33 | <23.11±0.34 | 12.17 ±0.33 |
| 15 | ${}^{14}_{\Lambda}C \rightarrow {}^7_3Li + {}^3_1H + {}^3_2He + n$ | 13198.86±0.34 | 13213.03±0.33 | 26.31±0.31 | 12.17 ±0.33 |
| 16 | ${}^{14}_{\Lambda}C \rightarrow {}^7_3Li + {}^3_2He + {}^3_1H + n$ | 13178.76±0.34 | 13213.03±0.33 | 46.41±0.34 | 12.17 ±0.33 |
| 17 | ${}^{14}_{\Lambda}C \rightarrow {}^3_1H + {}^7_3Li + {}^3_2He + n$ | 13202.85±0.34 | 13213.03±0.33 | 22.32±0.34 | 12.17 ±0.33 |
| 18 | ${}^{14}_{\Lambda}C \rightarrow {}^3_2He + {}^7_3Li + {}^3_1H + n$ | 13182.22±0.34 | 13213.03±0.33 | 42.95±0.34 | 12.17 ±0.33 |
| 19 | ${}^{14}_{\Lambda}C \rightarrow {}^7_3Li + {}^2_1H + {}^3_2He + 2n$ | >13160.34±0.34 | 13213.03±0.33 | <64.83±0.34 | 12.17 ±0.33 |
| 20 | ${}^{14}_{\Lambda}C \rightarrow {}^7_3Li + {}^3_2He + {}^2_1H + 2n$ | >13144.69±0.36 | 13213.03±0.33 | <80.48±0.36 | 12.17 ±0.33 |
| 21 | ${}^{14}_{\Lambda}C \rightarrow {}^2_1H + {}^7_3Li + {}^3_2He + 2n$ | >13162.64±0.34 | 13213.03±0.33 | <62.53±0.34 | 12.17 ±0.33 |

| No. | Possible Decay Modes | Calculated Mass(MeV/c ²) | Known Mass(MeV/c) | Calculated BE(MeV) | Known BE(MeV) |
|-----|--|--------------------------------------|-------------------|--------------------|---------------|
| 22 | ${}^{14}_{\Lambda}\text{C} \rightarrow {}^3_2\text{He} + {}^7_3\text{Li} + {}^2_1\text{H} + 2\text{n}$ | >13146.58±0.36 | 13213.03±0.33 | <78.59±0.36 | 12.17 ±0.33 |
| 23 | ${}^{14}_{\Lambda}\text{C} \rightarrow {}^7_3\text{Li} + {}^2_1\text{H} + {}^4_2\text{He} + \text{n}$ | 13201.95±0.34 | 13213.03±0.33 | 23.22±0.34 | 12.17 ±0.33 |
| 24 | ${}^{14}_{\Lambda}\text{C} \rightarrow {}^7_3\text{Li} + {}^4_2\text{He} + {}^2_1\text{H} + \text{n}$ | 13161.89±0.36 | 13213.03±0.33 | 63.28±0.36 | 12.17 ±0.33 |
| 25 | ${}^{14}_{\Lambda}\text{C} \rightarrow {}^2_1\text{H} + {}^7_3\text{Li} + {}^4_2\text{He} + \text{n}$ | 13206.08±0.34 | 13213.03±0.33 | 19.09±0.34 | 12.17 ±0.33 |
| 26 | ${}^{14}_{\Lambda}\text{C} \rightarrow {}^4_2\text{He} + {}^7_3\text{Li} + {}^2_1\text{H} + \text{n}$ | 13164.97±0.36 | 13213.03±0.33 | 60.20±0.36 | 12.17 ±0.33 |
| 27 | ${}^{14}_{\Lambda}\text{C} \rightarrow {}^7_3\text{Li} + {}^1_1\text{H} + {}^4_2\text{He} + 2\text{n}$ | >13151.33±0.34 | 13213.03±0.33 | <73.84±0.34 | 12.17 ±0.33 |
| 28 | ${}^{14}_{\Lambda}\text{C} \rightarrow {}^7_3\text{Li} + {}^4_2\text{He} + {}^1_1\text{H} + 2\text{n}$ | >13125.07±0.34 | 13213.03±0.33 | <100.84±0.34 | 12.17 ±0.33 |
| 29 | ${}^{14}_{\Lambda}\text{C} \rightarrow {}^1_1\text{H} + {}^7_3\text{Li} + {}^4_2\text{He} + 2\text{n}$ | >13153.70±0.34 | 13213.03±0.33 | <71.47±0.34 | 12.17 ±0.33 |
| 30 | ${}^{14}_{\Lambda}\text{C} \rightarrow {}^4_2\text{He} + {}^7_3\text{Li} + {}^1_1\text{H} + 2\text{n}$ | >13126.75±0.34 | 13213.03±0.33 | <98.42±0.34 | 12.17 ±0.33 |
| 31 | ${}^{15}_{\Lambda}\text{N} \rightarrow {}^9_4\text{Be} + {}^3_2\text{He} + {}^2_1\text{H} + \text{n}$ | 14141.58±0.19 | 14142.34±0.16 | 14.31±0.19 | 13.59±0.15 |
| 32 | ${}^{15}_{\Lambda}\text{N} \rightarrow {}^9_4\text{Be} + {}^1_1\text{H} + {}^3_2\text{He} + 2\text{n}$ | >14104.82±0.17 | 14142.34±0.16 | <51.07±0.17 | 13.59±0.15 |
| 33 | ${}^{15}_{\Lambda}\text{N} \rightarrow {}^9_4\text{Be} + {}^3_2\text{He} + {}^1_1\text{H} + 2\text{n}$ | >14086.32±0.19 | 14142.34±0.16 | <69.57±0.17 | 13.59±0.15 |
| 34 | ${}^{15}_{\Lambda}\text{N} \rightarrow {}^1_1\text{H} + {}^9_4\text{Be} + {}^3_2\text{He} + 2\text{n}$ | >14109.32±0.17 | 14142.34±0.16 | <46.57±0.19 | 13.59±0.15 |
| 35 | ${}^{15}_{\Lambda}\text{N} \rightarrow {}^3_2\text{He} + {}^9_4\text{Be} + {}^1_1\text{H} + 2\text{n}$ | >14090.34±0.19 | 14142.34±0.16 | <65.55±0.19 | 13.59±0.15 |
| 36 | ${}^{15}_{\Lambda}\text{N} \rightarrow {}^9_4\text{Be} + {}^4_2\text{He} + {}^1_1\text{H} + \text{n}$ | 14121.44±0.19 | 14142.34±0.16 | 34.45±0.19 | 13.59±0.15 |
| 37 | ${}^{15}_{\Lambda}\text{N} \rightarrow {}^4_2\text{He} + {}^9_4\text{Be} + {}^1_1\text{H} + \text{n}$ | 14128.49±0.19 | 14142.34±0.16 | 27.40±0.19 | 13.59±0.15 |
| 38 | ${}^{15}_{\Lambda}\text{N} \rightarrow {}^{10}_4\text{Be} + {}^3_2\text{He} + {}^1_1\text{H} + \text{n}$ | 14181.35±0.17 | 14142.34±0.16 | 14.53±0.19 | 13.59±0.15 |
| 39 | ${}^{15}_{\Lambda}\text{N} \rightarrow {}^{11}_5\text{B} + {}^1_1\text{H} + {}^1_1\text{H} + 2\text{n}$ | >14107.44±0.17 | 14142.34±0.16 | <56.00±0.17 | 13.59±0.15 |
| 40 | ${}^{15}_{\Lambda}\text{N} \rightarrow {}^1_1\text{H} + {}^{11}_5\text{B} + {}^1_1\text{H} + 2\text{n}$ | >14402.84±0.18 | 14142.34±0.16 | <48.45±0.17 | 13.59±0.15 |

Results and Discussions

A single- Λ hypernucleus event of J-PARC E07 experiment is analyzed in the present paper. The experimental data are supported by Professor Nakazawa who is the Spokesperson of J-PARC E07 experiment. Analysis is started from decay point B of analyzed event. Neutral particle emission at point B is firstly checked by dot product of direction vector of hyperfragment and total momentum of decay products. It is found that the angle between direction vector and total momentum is not equal to zero and neutral particle emission at point B is observed. Therefore, 85 possible decay modes with neutral particle decay products of track #1 single- Λ hypernucleus are chosen. In order to check the possible decay modes are allowed or forbidden, Q-values at point B are calculated and it is found that all 85 decay modes are allowed in nuclear emulsion. Then, the total energies of decay products are calculated. Total energies mean that the sum of kinetic energies of charged particle and that of neutral particles decay products. The Q-values and total energies are compared in table 2. According to table 2, we have found that 40 acceptable decay modes in which E_{total} are consistent with Q value within 3σ value. Moreover, mass and binding energy of track #1 single- Λ hypernucleus for all possible decay modes are calculated by mass-energy relation

and hypernuclei binding energy formula. The results are summarized in table 3. According to table 2 and table 3, ${}^{15}_{\Lambda}\text{N} \rightarrow {}^9_4\text{Be} + {}^3_2\text{He} + {}^2_1\text{H} + n$ decay mode has comparable Q-value and E_{total} in which 125.93 ± 0.16 MeV Q-value and 125.17 ± 0.03 MeV E_{total} value. Moreover, it is observed that the calculated mass of single- Λ hypernucleus is 14141.58 ± 0.19 MeV/ c^2 . This value is consistent with the known experimental mass 14142.34 ± 0.16 MeV/ c^2 of ${}^{15}_{\Lambda}\text{N}$ hypernucleus. Furthermore, the calculated binding energy for ${}^{15}_{\Lambda}\text{N}$ hypernucleus is found to be 14.31 ± 0.19 MeV which is very consistent with known binding energy value 13.59 ± 0.15 MeV. Therefore, ${}^{15}_{\Lambda}\text{N} \rightarrow {}^9_4\text{Be} + {}^3_2\text{He} + {}^2_1\text{H} + n$ decay mode is chosen as the acceptable decay mode of single- Λ hypernucleus track #1.

Moreover, ${}^{15}_{\Lambda}\text{N} \rightarrow {}^{10}_4\text{Be} + {}^3_2\text{He} + {}^1_1\text{H} + n$ decay mode has comparable Q-value and E_{total} in which 130.51 ± 0.16 MeV Q-value and 129.53 ± 0.03 MeV E_{total} value. Moreover, it is observed that the calculated mass of single- Λ hypernucleus is 14141.36 ± 0.19 MeV/ c^2 . This value is consistent with the known experimental mass 14142.34 ± 0.16 MeV/ c^2 of ${}^{15}_{\Lambda}\text{N}$ hypernucleus. Furthermore, the calculated binding energy for ${}^{15}_{\Lambda}\text{N}$ hypernucleus is found to be 14.53 ± 0.19 MeV which is very consistent with known binding energy value 13.59 ± 0.15 MeV. Therefore, ${}^{15}_{\Lambda}\text{N} \rightarrow {}^{10}_4\text{Be} + {}^3_2\text{He} + {}^1_1\text{H} + n$ decay mode is also chosen as the acceptable decay mode of single- Λ hypernucleus track #1. But, in the decay mode ${}^{15}_{\Lambda}\text{N} \rightarrow {}^{10}_4\text{Be} + {}^3_2\text{He} + {}^1_1\text{H} + n$, ${}^{10}_4\text{Be}$ is unstable particle and these decay mode is rejected.

Finally, a single- Λ hypernucleus track #1 is uniquely identified as ${}^{15}_{\Lambda}\text{N}$ which has 14141.58 ± 0.19 MeV/ c^2 mass and 14.31 ± 0.19 MeV binding energy value. The most probable decay mode is found as ${}^{15}_{\Lambda}\text{N} \rightarrow {}^9_4\text{Be} + {}^3_2\text{He} + {}^2_1\text{H} + n$ in which 125.93 ± 0.16 MeV energy is released for this decay mode.

Conclusions

A single- Λ hypernucleus event of J-PARC E07 experiment is analyzed kinematically. According to our analysis, a single- Λ hypernucleus track #1 is uniquely identified as ${}^{15}_{\Lambda}\text{N}$. The Q-values of decay mode, total energy, mass and binding energy of ${}^{15}_{\Lambda}\text{N}$ hypernucleus is obtained in this analysis. The results are very useful for hypernuclear identification research work. We can support the identification data to extend the nuclear chart with strangeness.

Acknowledgements

The authors would like to thank Lieutenant Colonel Saw Myint Oo, Dean of Faculty of Physics, Defence Services Academy for his encouragement and permission to complete this work. The authors also would like to thank all collaborators of KEK-PS E373 experiment for their discussions, supports and valuable advices to carry out hypernuclear research.

References

- Bando H., *et al.*, (1990), International Journal of Modern Physics **A5**, pp. 4021-4198
 Ichikawa A., *et al.*, (2001), Physical Review Letters **B500**.
 Nakazawa K., (2018), Private Communication.
 Nakazawa K., *et al.*, (2013), Physical Review Letters **C 88**.
 Samanta C., and Schmitt A. T., (2019), "AIP Conference Proceedings, Vol. 2130, pp. 040004.
 Takahashi T., *et al.*, (2012) Progress of Theoretical and Experimental Physics 02B010.